Transition Metal Chemistry **28**: 548–557, 2003.
© 2003 *Kluwer Academic Publishers. Printed in the Netherlands.*

Hydrogen-bonded networks based on manganese(II), nickel(II), copper(II) and zinc(II) complexes of *N*,*N*′-dimethylurea

Robby Keuleers and Herman O. Desseyn
Department of Chemistry, University of Antwerp, RUCA, Groenenborgerlaan 171, 2020 Antwerp, Belgium

Giannis S. Papaefstathiou, Labrini Drakopoulou and Spyros P. Perlepes*
Department of Chemistry, University of Patras, 265 04 Patras, Greece

Catherine P. Raptopoulou and Aris Terzis
Institute of Materials Science, NCSR 'Demokritos', 153 10 Aghia Paraskeri Attikis, Greece

Received 19 August 2002; accepted 10 October 2002

Abstract

A project related to the crystal engineering of hydrogen-bonded coordination complexes has been initiatied and some of our first results are presented here. The compounds $[Mn(DMU)_6](ClO_4)_2$ *(1)*, $[Ni(DMU)_6](ClO_4)_2$ *(2)*, $[Cu(OClO_3)_2(DMU)_4]$ *(3)* and $[Zn(DMU)_6](ClO_4)_2$ *(4)* have all been prepared from the reaction of *N*,*N*′-dimethylurea (DMU) and the appropriate hydrated metal perchlorate salt. Crystal structure determinations of the four compounds demonstrate the existence of $[M(DMU)_6]^{2+}$ cations and ClO_4^- counterions in *(1)*, *(2)* and *(4)*, whereas in *(3)* monodentate coordination of the perchlorate groups leads to molecules. The $[M(DMU)_6]^{2+}$ cations and ClO_4^- anions self-assemble to form a hydrogen-bonded one-dimensional (1D) architecture in *(1)* and different 2D hydrogen-bonded networks in *(2)* and *(4)*. The hydrogen bonding functionalities on the molecules of *(3)* create a 2D structure. The complexes were also characterised by room-temperature effective magnetic moments and i.r. studies. The data are discussed in terms of the nature of bonding and the known structures.

Introduction

At an early stage, children are fascinated with building blocks and LEGOs because elaborate structures may be created from far simpler objects [1]. It is with the same enthusiasm and fascination that chemists have approached the idea of employing molecular building blocks to assemble non-covalent structures. This straightforward concept, self-assembly, is the basis of supramolecular chemistry [2, 3] and is likely to play a key role in the advancement of the emerging field of nanotechnology.

Because of their strength and directionality, hydrogen bonds are an ideal 'glue' for the assembly of molecular building blocks through non-covalent interactions [1]. A variety of elegant hydrogen-bonded supramolecules has been reported [4–10], including engineered crystals and liquid crystals. However, the number of hydrogen-bonded modules available for use by supramolecular chemists is, to an extent, limited [1].

Hydrogen bonding in organic crystals has been established as a reliable force for organic crystal engineering [10–12], but it has only recently been introduced as a tool for the supramolecular assembly of coordination complexes by Mingos and coworkers [13], and other groups [14–23]. These groups studied the efficacy of the hydrogen bond in the crystal engineering of transition-metal systems. By reacting metal ions with ligands that contain both efficient metal coordination sites and peripheral hydrogen bonding functionalities, assembly can be dictated by intermolecular hydrogen bonding interactions.

We have recently become interested in the crystal engineering of hydrogen-bonded coordination complexes [24, 25]. Our emphasis is on coordination complexes with peripheral hydrogen bonding substituents that cannot coordinate to the metal ions. Our short-term goal is to create novel supramolecular structures based on hydrogen bonding interactions between *simple* metal complexes. This project can be regarded as an extension of our work in the area of coordination polymers [26–29]. At this point we feel that it is appropriate to highlight the analogies [30] that can be drawn between hydrogen-bonded networks and coordination polymers. In particular, for hydrogen-bonded networks the donor (*i.e.* a protic hydrogen atom) and the acceptor (*i.e.* a region of electron density) can be compared with metal ions and ligands, respectively.

Furthermore, as noted by Etter [31], in cases where there are multiple hydrogen bonding sites, there is a rather good degree of predictability concerning which donors and acceptors will engage. Therefore, the 'node

* Author for correspondence

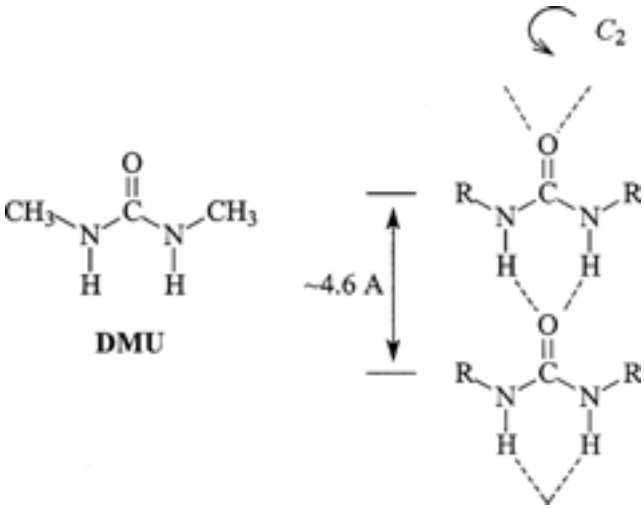

Fig. 1. *N*,*N*′-dimethylurea (DMU) and a small portion (which contains only two molecules) of the α-network commonly observed in symmetrical disubstituted ureas (right).

and spacer' approach can be employed equally well with hydrogen bonds as with coordination bonds [30].

This paper describes the full physical, spectroscopic and structural characterisation of the products from the reactions between manganese(II), nickel(II), copper(II) and zinc(II) perchlorates with *N*,*N*′-dimethylurea (DMU, Figure 1). Ureas are superb hydrogen bonding molecules [1, 32, 33]. Symmetrical disubstituted ureas, like DMU, form α-networks with each urea molecule donating two hydrogen bonds, 'chelating' the carbonyl oxygen of the next molecule in the network (Figure 1). In crystals, ureas commonly have C_2 point group symmetry; the mirror planes are almost always lost. The resulting α-networks tend to have $P\bar{2}$ rod symmetry with a characteristic intermolecular spacing of ~4.6 Å [33, 34[1]]. In contrast to the great number of studies concerning free ureas [1, 7, 8, 32, 33, 35], little is known about the supramolecular structures based on hydrogen bonding interactions between simple metal–ureas complexes. We were interested in studying the supramolecular structures of simple metal–DMU complexes where, in principle, the oxygen atom of DMU can coordinate to the metal ion and/or provide a hydrogen bonding acceptor site. To exclude the possibility of coordination polymer formation through anionic ligands, we employed metal sources containing the perchlorate ion which is normally not coordinated. Thus, infinite assemblies based on ligand–counterion hydrogen bonds were expected, though these are not, strictly speaking, ligand-based hydrogen-bonded assemblies. The present work can be also regarded as a continuation of our effort in the spectroscopy of free ureas [36, 37] and in the study of their coordination chemistry [38–40].

Experimental

General and physical measurements

All manipulations were performed under aerobic conditions using solvents as received. Perchlorate salts and *N*,*N*′-dimethylurea (DMU) were purchased from Aldrich Co. Elemental analyses (C,H,N) were performed by the University of Ioannina (Greece) Microanalytical Laboratory using an EA 1108 Carlo Erba analyser. I.r. spectra (4000–500 cm^{-1}) were recorded on a Perkin-Elmer 16 PC Fourier-transform (FT) spectrometer with samples prepared as KBr pellets, and on a Bruker IFS 113v FT spectrometer with samples prepared as Nujol mulls between CsI plates. Room temperature magnetic susceptibility measurements were carried out by Faraday's method using a Cahn–Ventron RM-2 balance standardised with $HgCo(NCS)_4$. Diamagnetic corrections were estimated from Pascal's constants.

Compound preparation

Complexes $[Mn(DMU)_6](ClO_4)_2$ *(1)*, $[Ni(DMU)_6](ClO_4)_2$ *(2)*, $[Cu(OClO_3)_2(DMU)_4]$ *(3)* and $[Zn(DMU)_6](ClO_4)_2$ *(4)* were all prepared similarly. A solution of $M(ClO_4)_2 \cdot 6H_2O$ (1.0 mmol, M = Mn, Ni, Cu, Zn) in EtOH (10 cm^3) was added to a solution of DMU (7.0 mmol) in the same solvent (10 cm^3). No noticeable colour change occurred. The solution obtained was stirred for 5 min and then layered with an equal vol of a mixture of Et_2O and *n*-hexane (50:50, v/v). Slow mixing gave crystals of the products (suitable for single-crystal X-ray crystallography), which were collected by filtration, washed with a small amount of cold EtOH and Et_2O, and dried *in vacuo* over silica gel. The same complexes could also be prepared using Me_2CO as the reaction solvent. Complex *(3)* was also prepared by reacting $Cu(ClO_4)_2 \cdot 6H_2O$ with 2, 4, 6 or 8 equivalents of DMU in THF under a variety of crystallisation conditions (layering with Et_2O, *n*-hexane, Et_2O/*n*-hexane, refrigerator). Yields, colours, analytical results and effective magnetic moments for the prepared new complexes are given in Table 1.

Caution: *Perchlorate salts are potentially explosive. Although no detonation tendencies have been observed in our experiments, caution is advised and handling of only small quantities is recommended.*

X-ray crystallographic studies[2]

Suitable crystals of *(1)*, *(2)*, *(3)* and *(4)* were mounted in air. Diffraction measurements of *(1)* and *(4)* were

[1] Supramolecular assemblies are classified into four groups depending upon the degree of translation symmetry, see Ref. [34]. An α-network has one degree of translation symmetry and is characterised by its rod group symmetry.

[2] CCDC codes 188960, 188961, 188962 and 188963 for complexes *(1)*, *(2)*, *(3)* and *(4)*, respectively.

Table 1. Yields, colours, analytical results and effective magnetic moments for the new manganese(II), nickel(II), copper(II) and zinc(II) complexes of *N*,*N'*-dimethylurea

Complex	Yield[a,b] (%)	Colour	Found (calcd.) (%) C	H	N	μ_{eff} (B.M.)[c,d]
$[Mn(DMU)_6)](ClO_4)_2$ *(1)*	53	cream	27.4 (27.6)	6.1 (6.2)	21.7 (21.5)	6.02
$[Ni(DMU)_6](ClO_4)_2$ *(2)*	58	pale green	27.3 (27.5)	6.1 (6.2)	21.2 (21.4)	3.11
$[Cu(OClO_3)_2(DMU)_4]$ *(3)*	56	light blue	23.6 (23.4)	5.2 (5.2)	18.3 (18.2)	1.99
$[Zn(DMU)_6](ClO_4)_2$ *(4)*	70	white	27.5 (27.3)	6.0 (6.1)	21.2 (21.2)	Dia

Dia = diamagnetic.
[a] Based on the metal; [b] the quoted values are from preparations with Me_2CO as solvent (the yields from the preparations in EtOH are lower); [c] per metal ion; [d] at room temperature.

Table 2. Crystallographic data for complexes *(1)*, *(2)*, *(3)* and *(4)*

Parameter	*(1)*	*(2)*	*(3)*	*(4)*
Color (habit)	Colourless prisms	Pale green prisms	Light blue prisms	Colourless prisms
Crysal size (mm)	0.20 × 0.20 × 0.40	0.10 × 0.10 × 0.40	0.10 × 0.20 × 0.50	0.10 × 0.20 × 0.50
Chemical formula	$C_{18}H_{48}MnN_{12}O_{14}Cl_2$	$C_{18}H_{48}NiN_{12}O_{14}Cl_2$	$C_{12}H_{32}CuN_8O_{12}Cl_2$	$C_{18}H_{48}ZnN_{12}O_{14}Cl_2$
M	782.52	786.29	614.90	792.95
Crystal system	Triclinic	Triclinic	Monoclinic	Triclinic
Space group	P1	P1	$P2_1/c$	P1
Unit cell dimensions				
a (Å)	8.043(1)	8.022(8)	10.109(4)	8.024(1)
b (Å)	10.741(2)	10.66(1)	8.550(4)	11.642(1)
c (Å)	11.713(2)	11.63(1)	14.978(7)	10.662(1)
α (Å)	68.54(1)	68.60(3)		68.65(1)
β (Å)	81.51(1)	81.11(3)	98.77(1)	81.94(1)
γ (Å)	81.93(5)	81.70(3)		81.29(1)
V (Å^3)	927.3(3)	911(2)	1280(1)	913.1(1)
Z	1	1	2	1
D_{calc} (g cm^{-3})	1.401	1.433	1.596	1.442
μ (mm^{-1})	4.859	0.752	1.132	2.930
Radiation (Å)	CuK_α (1.54180)	MoK_α (0.71073)	MoK_α (0.71073)	CuK_α (1.54180)
Temperature (K)	298	298	298	298
Scan mode/speed (° min^{-1})	$\vartheta-2\vartheta$/3.0	$\vartheta-2\vartheta$/3.0	$\vartheta-2\vartheta$/3.8	$\vartheta-2\vartheta$/3.0
Scan range (°)	2.5 + $\alpha_1\alpha_2$ separation	2.4 + $\alpha_1\alpha_2$ separation	2.4 + $\alpha_1\alpha_2$ separation	2.5 + $\alpha_1\alpha_2$ separation
ϑ range (°)	4.4–62.5	1.9–25.0	2.0–26.0	4.5–65.0
Reflections collected	3183	3461	2626	3266
Unique reflections	2948 (R_{int} = 0.0108)	3211 (R_{int} = 0.0091)	2522 (R_{int} = 0.0320)	3086 (R_{int} = 0.0113)
Reflections used [$I > 2\sigma(I)$]	2595	2815	2152	2824
Parameters refined	290	338	225	339
$[\Delta/\sigma]_{max}$	0.149	0.182	0.049	0.218
$[\Delta\rho]_{max}/[\Delta\rho]_{min}$ (e Å^{-3})	0.653/−0.427	0.330/−0.348	0.405/−0.493	0.329/−0.361
w[a]	a = 0.0959, b = 0.5902	a = 0.0483, b = 0.2714	a = 0.0489, b = 0.5878	a = 0.619, b = 0.3189
GoF (on F^2)	1.071	1.032	1.052	1.049
R_1^b	0.0544	0.0362	0.0354	0.0386
wR_2^c	0.1585	0.0970	0.0949	0.1069

[a] $w = 1/[\sigma^2(F_c^2) + (aP)^2 + bP]$ with $P = (\max(F_o^2,0) + 2F_c^2)/3$; [b] $R_1 = \sum(|F_o|-|F_c|)/\sum(|F_o|)$; [c] $wR_2 = \{\sum[w(F_o^2-F_c^2)^2]/\sum[w(F_o^2)^2]\}^{1/2}$.

made on a P21 Nicolet diffractometer using Ni-filtered Cu radiation, while for *(2)* and *(3)* a Crystal Logic dual goniometer diffractometer using graphite-monochromated Mo radiation was employed. Crystal data and full details of the data collection and data processing are listed in Table 2. Unit cell dimensions were determined and refined by using three angular settings of 25 automatically centred reflections in the ranges 24° < 2ϑ < 54° for *(1)* and *(4)*, and 11° < 2ϑ < 23° for *(2)* and *(3)*. Three standard reflections, monitored every 97 reflections, showed less than 3% intensity fluctuation and no decay. Lorentz, polarisation and Ψ-scan absorption corrections were applied for *(1)* and *(4)*, while only the first two corrections were applied for *(2)* and *(3)*, using Crystal Logic software.

The structures were solved by direct methods using SHELXS-86 [41] and refined by full-matrix least-squares on F^2 with SHELXL-93 [42]. For all structures, all non-H atoms were refined using anisotropic thermal parameters, except perchlorate oxygens O(3), O(4) and O(5) for *(2)* which were found disordered and refined anisotropically in two orientations with occupation

factors free to vary and perchlorate oxygens O(3), O(4) and O(5) for *(4)* which were also found disordered and refined anisotropically in two orientations with occupancies 53 and 46%. All H-atoms were located by difference maps, except those on C(13) and C(23) of *(1)* which were introduced at calculated positions as riding on their bonded atoms, and refined isotropically.

Results and discussion

Preparation of the complexes

The preparation of the four complexes is summarised by Equations (1) and (2):

$$\mathrm{M(ClO_4)_2 \cdot 6H_2O + 6DMU} \xrightarrow[\mathrm{M=Mn,\ Ni,\ Zn}]{\mathrm{EtOH\ or\ Me_2CO}} \underset{(1),(2),(4)}{[\mathrm{M(DMU)_6}](\mathrm{ClO_4})_2} + \mathrm{6H_2O} \quad (1)$$

$$\mathrm{Cu(ClO_4)_2 \cdot 6H_2O + 4DMU} \xrightarrow[\mathrm{or\ THF}]{\mathrm{EtOH\ or\ Me_2CO}} \underset{(3)}{[\mathrm{Cu(OClO_3)_2(DMU)_4}]} + \mathrm{6H_2O} \quad (2)$$

Complexes *(1)–(4)* seem to be the only products from the $M(ClO_4)_2 \cdot 6H_2O$/DMU reaction systems (M = Mn, Ni, Cu, Zn). The solvent and the DMU:M^{II} reaction ratio have no influence on the identity of the complexes.

Description of structures

Selected bond distances and angles for complexes *(1)*, *(2)* and *(3)* are listed in Tables 3–5, respectively. ORTEP plots of the cations $[Mn(DMU)_6]^{2+}$ and $[Ni(DMU)_6]^{2+}$ present in complexes *(1)* and *(2)* are shown in Figures 2 and 3, respectively; the molecular structure of *(3)* is depicted in Figure 4. Details of the hydrogen bonds of *(1)*, *(2)* and *(3)* are provided in Tables 6, 7 and 8, respectively.

Complexes *(1)*, *(2)* and *(4)* crystallise in triclinic space group $P\bar{1}$ and are isostructural. Their structures consist of almost perfect octahedral $[M(DMU)_6]^{2+}$ cations and ClO_4^- counterions. The metal ion sits on an inversion centre and is surrounded by six O-bonded DMU ligands. There are six strong intramolecular (intracationic) hydrogen bonds inside each cation with atoms N(1), N(11) and N(21) (and their symmetry equivalents) as donors, and atoms O(1), O(11) and O(21) (and their symmetry equivalents) as acceptors.

The structure of *(3)* consists of $[Cu(OClO_3)_2(DMU)_4]$ molecules. The molecule of this complex has a crystallographically imposed inversion centre and the Cu^{II} atom is coordinated by four monodentate DMU molecules and two monodentate perchlorato ligands. Due to the Jahn–Teller effect, the axial Cu—O($OClO_3$) bonds are weak [2.584(2) Å]. There are six intramolecular hydrogen bonds, two of them being bifurcated. Each perchlorato ligand accepts [through O(2) and O(4)] two hydrogen bonds from a single N(2)—H donor group (bifurcated hydrogen bond), while each DMU O(1) atom accepts a strong hydrogen bond from the N(12)—H group belonging to a different DMU ligand. Finally there are two (symmetry equivalent) C(11)—H(11A)···O(11) interactions that can be regarded as weak hydrogen bonds. The directional properties of C—H···O bonds have been exploited by Weber and

Table 3. Selected bond lengths (Å) and angles (°) for complex *(1)*[a]

Bond lengths			
Mn(1)—O(1)	2.160(2)	C(12)—O(11)	1.241(4)
Mn(1)—O(11)	2.170(2)	C(12)—N(11)	1.341(5)
Mn(1)—O(21)	2.175(2)	C(12)—N(12)	1.326(5)
C(2)—O(1)	1.259(4)	C(22)—O(21)	1.258(4)
C(2)—N(1)	1.329(5)	C(22)—N(21)	1.335(5)
C(2)—N(2)	1.323(5)	C(22)—N(22)	1.323(5)
Bond angles			
O(1)—Mn—O(11)	91.6(1)	C(2)—O(1)—Mn	131.6(2)
O(1)—Mn—O(21)	89.9(1)	C(12)—O(11)—Mn	128.1(2)
O(11)—Mn—O(21)	90.1(1)	C(22)—O(21)—Mn	129.9(2)

[a] Atoms C(2), C(12) and C(22), which are not labelled in Figure 2, are the carbonyl carbon atoms of the three crystallographically independent DMU molecules.

Table 4. Selected bond lengths (Å) and angles (°) for complex *(2)*[a]

Bond lengths			
Ni—O(1)	2.059(2)	C(12)—O(11)	1.260(3)
Ni—O(11)	2.065(2)	C(12)—N(11)	1.323(3)
Ni—O(21)	2.069(3)	C(12)—N(12)	1.342(4)
C(2)—O(1)	1.265(3)	C(22)—O(21)	1.256(3)
C(2)—N(1)	1.331(3)	C(22)—N(21)	1.334(4)
C(2)—N(2)	1.327(3)	C(22)—N(22)	1.337(3)
Bond angles			
O(1)—Ni—O(11)	92.5(1)	C(2)—O(1)—Ni	131.1(2)
O(1)—Ni—O(21)	91.5(1)	C(12)—O(11)—Ni	129.0(2)
O(11)—Ni—O(21)	91.3(1)	C(22)—O(21)—Ni	130.7(2)

[a] Atoms C(2), C(12) and C(22), which are not labelled in Figure 3, are the carbonyl carbon atoms of the three crystallographically independent DMU molecules.

Table 5. Selected bond lengths (Å) and angles (°) for complex *(3)*[a]

Bond lengths			
Cu—O(1)	1.936(2)	C(12)—N(11)	1.329(3)
Cu—O(11)	1.951(2)	C(12)—N(12)	1.324(4)
Cu—O(2)	2.584(2)	Cl—O(2)	1.436(2)
C(2)—O(1)	1.273(3)	Cl—O(3)	1.420(2)
C(2)—N(1)	1.328(3)	Cl—O(4)	1.423(2)
C(2)—N(2)	1.321(4)	Cl—O(5)	1.409(3)
C(12)—O(11)	1.264(3)		
Bond angles			
O(1)—Cu—O(11)	86.9(1)	O(2)—Cl—O(4)	108.5(2)
O(1)—Cu—O(2)	90.2(1)	O(2)—Cl—O(5)	110.1(2)
O(11)—Cu—O(2)	91.8(1)	O(3)—Cl—O(4)	110.1(2)
C(2)—O(1)—Cu	132.6(2)	O(3)—Cl—O(5)	109.5(2)
C(12)—O(11)—Cu	134.5(2)	O(4)—Cl—O(5)	111.0(2)
O(2)—Cl—O(3)	107.6(2)		

[a] Atom C(12), which is not labelled in Figure 4, is the carbonyl carbon atom of one of the two crystallographically independent DMU molecules.

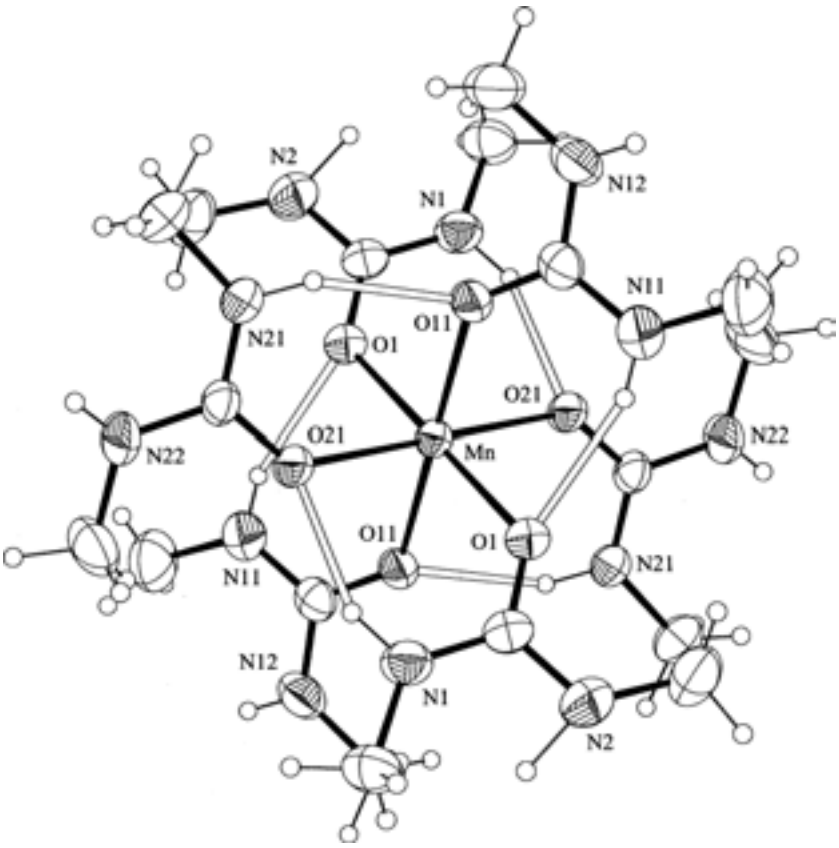

Fig. 2. An ORTEP representation of the cation $[Mn(DMU)_6]^{2+}$ present in complex *(1)*. Open bonds indicate intramolecular hydrogen bonds. An identical labeling scheme is used for atoms generated by symmetry. For clarity, all carbon atoms are not labelled.

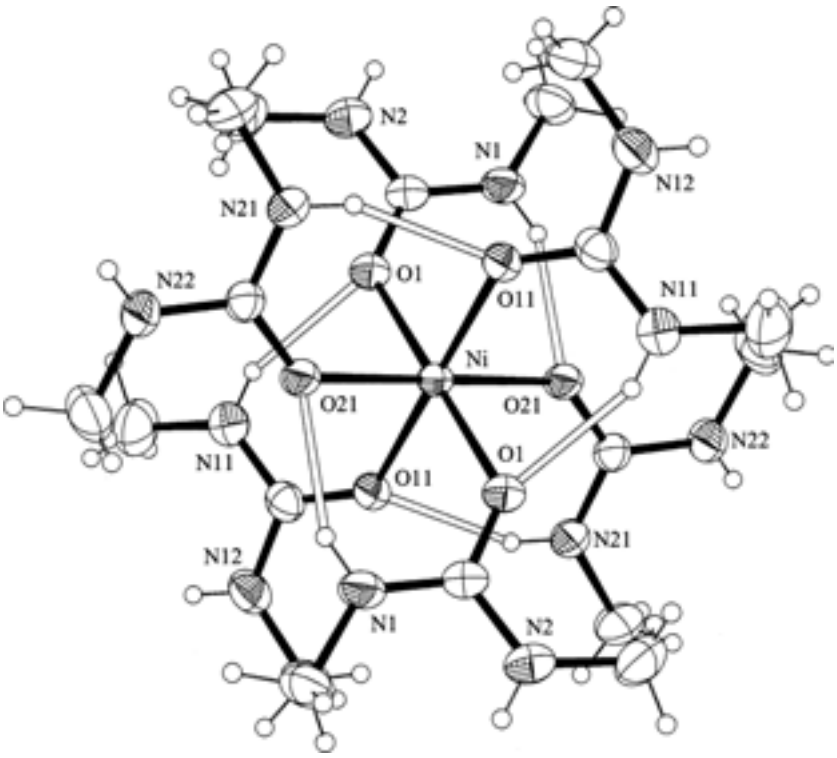

Fig. 3. An ORTEP representation of the cation $[Ni(DMU)_6]^{2+}$ present in complex *(2)*. Open bonds indicate intramolecular hydrogen bonds. An identical labeling scheme is used for atoms generated by symmetry. For clarity, all carbon atoms are not labelled.

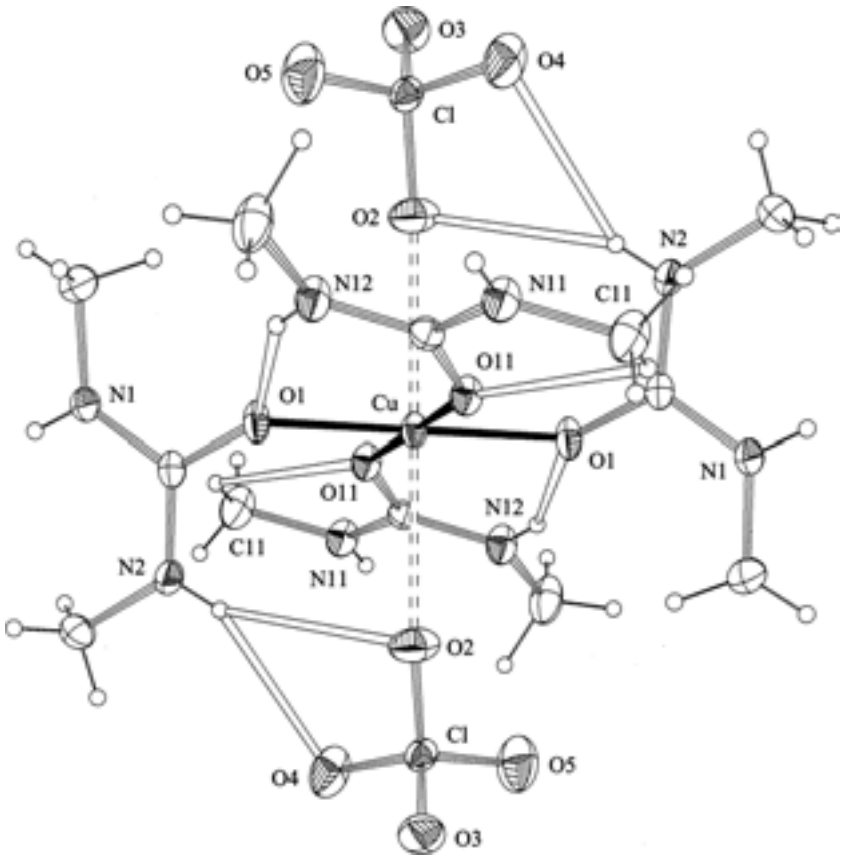

Fig. 4. The molecular structure of complex *(3)*. The double dashes indicate the weak axial copper(II)–perchlorate bonds. Open bonds indicate intramolecular hydrogen bonds. An identical labeling scheme is used for atoms generated by symmetry. For clarity, most carbon atoms are not labelled.

Table 6. Dimensions of the unique hydrogen bonds (distances in Å and angles in °) for complex *(1)*

D—H····A	D····A	H····A	∠DHA
N(1)—H(N1)····O(21)[a]	2.933(4)	2.07(5)	156(5)
N(11)—H(N11)····O(1)[a]	2.943(5)	2.06(5)	154(5)
N(21)—H(N21)····O(11)[a] 2.992(5)	2.20(5)	158(4)	
N(2)—H(N2)····O(3)[b] [1−*x*, −*y*, −*z*][c]	3.034(8)	2.31(5)	167(5)
N(12)—H(N12)····O (2)[b] [1−*x*, −1−*y*, 1−*z*][c]	3.148(7)	2.40(10)	121(6)

A = acceptor; D = donor.
[a] Intramolecular (intracationic) hydrogen bonds, see Figure 2; [b] these atoms belong to the perchlorate counterions not shown in Figure 2; [c] intermolecular (interionic) hydrogen bonds.

Table 7. Dimensions of the unique hydrogen bonds (distances in Å and angles in °) for complex *(2)*

D—H····A	D····A	H····A	∠DHA
N(1)—H(N1)····O(21)[a]	2.857(4)	2.07(3)	157(3)
N(11)—H(N11)····O(1)[a]	2.875(4)	2.11(3)	154(3)
N(21)—H(N21)····O(11)[a]	2.897(5)	2.14(3)	155(3)
N(2)—H(N2)····O(2)[b] [1−*x*, −*y*, −*z*][c]	3.013(5)	2.29(3)	167(3)
N(12)—H(N12)····O(3)[b] [1−*x*, −1−*y*, 1−*z*][c]	3.220(16)	2.53(5)	146(4)
N(12)—H(N12)····O(4A)[d] [1−*x*, −1−*y*,1−*z*][c]	3.092(16)	2.44(5)	141(4)
C(1)[e]—H(1B)····O(3)[b] [*x*, 1+*y*, −1+*z*][c]	3.275(14)	2.55(4)	136(3)
C(23)[e]—H(23C)····O(5)[b] [*x*, 1+*y*, −1+*z*][c]	2.980(16)	2.59(7)	108(5)

A = acceptor; D = donor.
[a] Intramolecular (intracationic) hydrogen bonds, see Figure 3; [b] these atoms belong to the perchlorate counterions, not shown in Figure 3; [c] intermolecular (interionic) hydrogen bonds; [d] disordered perchlorate oxygen atom;[e] these atoms belong to methyl groups of DMU ligands.

co-workers who designed carboxylic acid hosts that are capable of including DMF and DMSO as guests *via* specific recognition schemes [43, 44].

The M—O_{DMU} bond distances in *(1)–(4)* are comparable to those in manganese(II), nickel(II), copper(II) and zinc(II) complexes with urea-type ligands [38, 39, 45]. All DMU molecules in *(1)–(4)* are coordinated in a bent fashion, with M—O—C angles ranging from 128.1(2)° to 134.5(2)°. This is the usual way of coordination of urea and its derivatives [46]. Linearly or approximately linearly coordinated ureas have been observed only in a few cases [38, 46, 47].

The average M—O_{DMU} bond lengths change according to the sequence *(1)* [2.168 Å] > *(2)* [2.064 Å] > *(3)* [1.943 Å] < *(4)* [2.095 Å], *i.e.*, they follow the Irving–Williams series. The strong M—O_{DMU} bonds in *(3)* are reflected in the longer CO (average 1.268 Å) and shorter $C_{carbonyl}$—N bond distances in this complex, compared to *(1)*, *(2)* and *(4)*.

Complexes *(1)–(4)* extend to eight the number of structurally characterised metal complexes of DMU. The four, previously structurally characterised, complexes are $[Mn(NO_3)_2(DMU)_3]$ [38], $[MnBr_2(DMU)_3]$ [47], $[Fe(DMU)_6](ClO_4)_3$ [48] and $[Er(DMU)_6(H_2O)](ClO_4)_3$ [49].

Table 8. Dimensions of the unique hydrogen bonds (distances in Å and angles in °) for complex *(3)*

D—H····A	D····A	H····A	∠DHA
N (2)—H(N2)····O(2)[a]	3.216(4)	2.53(3)	155(3)
N(2)—H(N2)····O(4)[a]	3.146(4)	2.49(3)	150(3)
N(12)—H(N12)····O(1) [$-x$, $-y$, $1-z$][a]	2.784(3)	2.12(3)	152(3)
C(11)—H(11A)····O(11)[a]	2.741(4)	2.43(5)	105(4)
N(1)—H(N1)····O(3) [x, $1+y$, z][b]	3.140(4)	2.43(3)	158(3)
N(11)—H(N11)····O(4) [$1-x$, $-y$, $1-z$][b]	3.155(4)	2.48(3)	163(4)

A = acceptor; D = donor.
[a] Intramolecular hydrogen bonds, see Figure 4; [b] intermolecular hydrogen bonds.

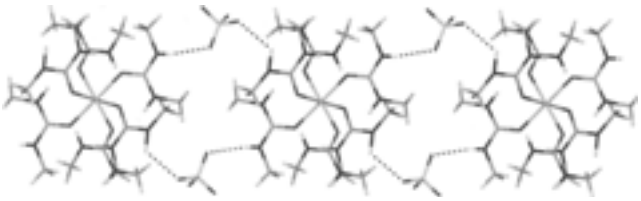

Fig. 5. A view of the 1D network formed by hydrogen bonding between $[Mn(DMU)_6]^{2+}$ cations and ClO_4^- counterions in complex *(1)*. Only the intermolecular (interionic) hydrogen bonds are shown.

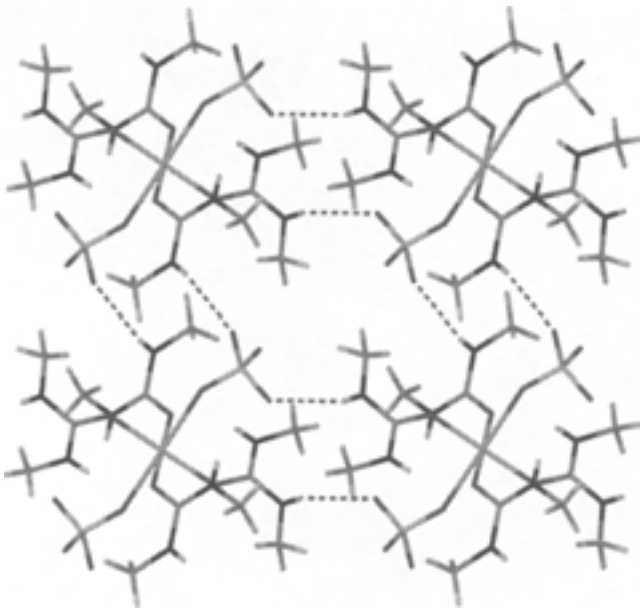

Fig. 7. A view of the 2D network formed by hydrogen bonding between the $[Cu(OClO_3)_2(DMU)_4]$ molecules in complex *(3)*. Only the intermolecular hydrogen bonds are shown.

We have up to now discussed aspects of the molecular structures of complexes *(1)–(4)*. Figures 5–8 provide views of the hydrogen-bonded networks of the complexes. Metric parameters for the intermolecular hydrogen bonds present in the crystal structures of *(1)–(3)* have been included in Tables 6–8.

In *(1)*, two oxygen atoms from each perchlorate, O(2) and O(3), act as hydrogen bond acceptors to NH groups from two DMU ligands belonging to two different $[Mn(DMU)_6]^{2+}$ cations; these ligand-counterion hydrogen bonds create infinite one-dimensional (1D) assemblies (Figure 5).

The crystal structure of *(2)* reveals an elegant hydrogen-bonded 2D network based on cations and anions (Figure 6). One dimension is created by two crystallographically independent N—H···O(ClO_4^-) interactions similar to those found in *(1)*, while the other dimension is achieved through the C(1)—H(1B)···O(3) $[x, 1+y, -1+z]$ interaction. Each perchlorate accepts four hydrogen bonds through three oxygen atoms.

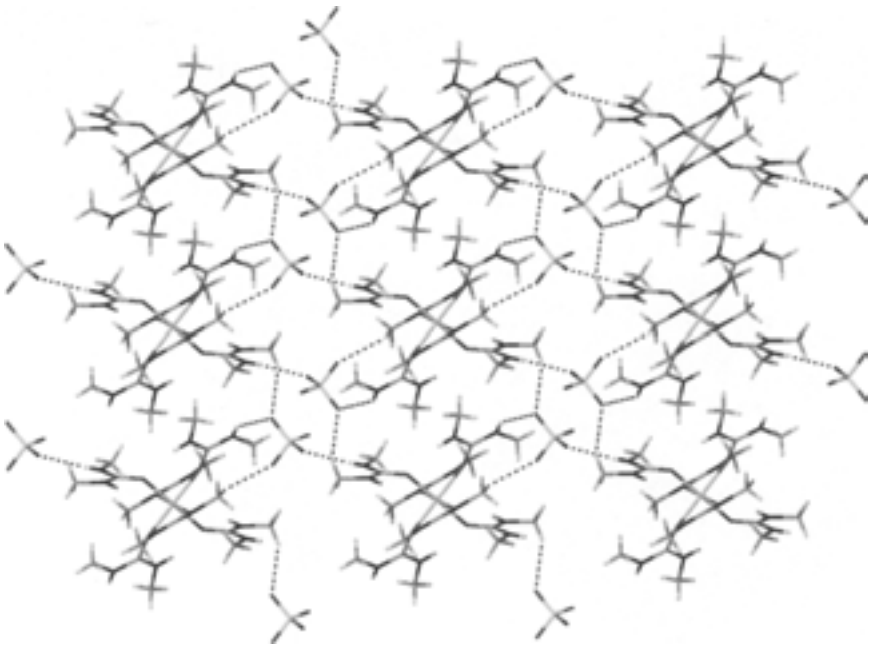

Fig. 6. A view of the 2D network formed by hydrogen bonding between $[Ni(DMU)_6]^{2+}$ cations and ClO_4^- counterions in complex *(2)*. Only the intermolecular (interionic) hydrogen bonds are shown. For clarity, the hydrogen bonds to disordered perchlorate oxygen atoms (see Table 7) have not been drawn.

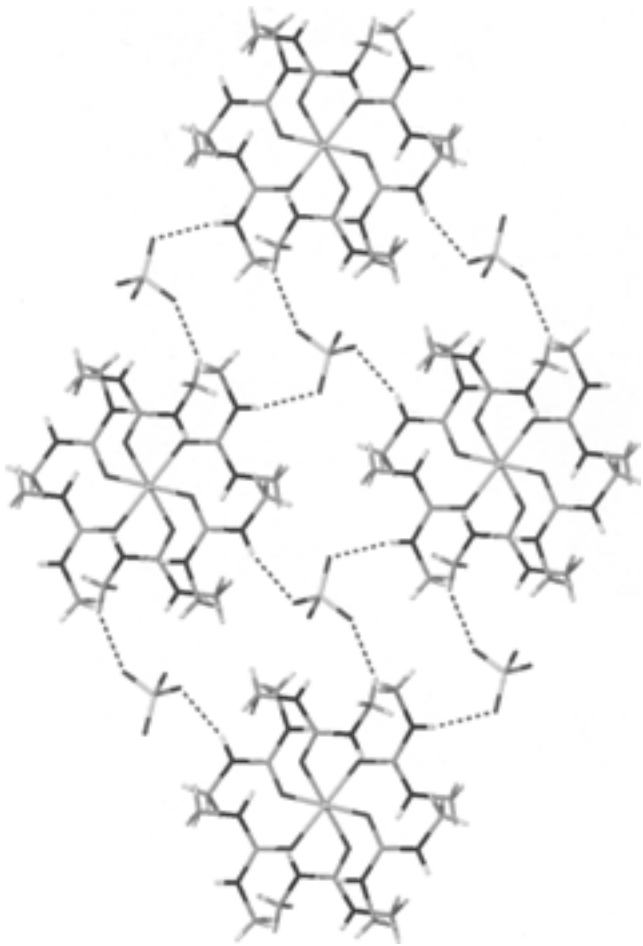

Fig. 8. A view of the 2D network formed by hydrogen bonding between $[Zn(DMU)_6]^{2+}$ cations and ClO_4^- counterions in complex *(4)*. Only the intermolecular (interionic) hydrogen bonds are shown. For clarity the hydrogen bonds to disordered perchlorate oxygen atoms are not shown.

The $[Cu(OClO_3)_2(DMU)_4]$ molecules in *(3)* are arranged in infinite 2D networks through two crystallographically independent intermolecular N—H···O(ClO_4^-) hydrogen bonds; thus each perchlorato ligand participates in two intramolecular and two intermolecular hydrogen bonds using three oxygen atoms, including the coordinated oxygen atom [O(2)].

The $[Zn(DMU)_6]^{2+}$ cations of *(4)* are linked through ClO_4^- counterions to generate a 2D network. One dimension is created by two crystallographically independent N—H···O(ClO_4^-) interactions similar to those observed in *(1)* and *(2)*, while the second dimension is achieved through one crystallographically unique C—H···O(ClO_4^-) interaction. Each ClO_4^- ion uses three oxygen atoms as hydrogen bond acceptors to NH groups from two DMU ligands belonging to different cations and to one methyl group of a third cation.

Physical and spectroscopic characterisation of the complexes

The room-temperature effective magnetic moment (μ_{eff}) of the complexes (Table 1) indicate that the manganese(II) complex is of the high-spin type, as expected. The value for *(2)* shows a small orbital contribution, in accord with its six-coordinate stereochemistry [50]. The value for the copper(II) complex *(3)* (1.99 B.M.) indicates that this is magnetically dilute.

The full vibrational analysis of crystalline DMU has been published [36]. Table 9 gives diagnostic i.r. bands of the free ligand and its metal complexes. Assignments in Table 9 have been given in comparison with the data obtained for the free ligand [36] and its complex $[Mn(NO_3)_2(DMU)_3]$ [38], and by studying literature reports [47, 51, 52]. The bands with $\nu(CN)_{amide}$ character are situated at higher frequencies in the spectra of *(1)–(4)* than for free DMU, whereas the ν(CO) band shows a frequency decrease. These shifts are consistent with oxygen coordination, suggesting the presence of $^+N{=}C{-}O^-$ resonant forms [47]. Upon coordination *via* oxygen, the positively charged metal ion stabilises the negative charge on the oxygen atom; the NCO function now occurs in its polar resonance form and, thus, the double bond character of the CN bond increases, while the double bond character of the CO bond decreases.

The i.r. spectra of complexes *(1)*, *(2)* and *(4)* in KBr pellets exhibit strong bands at ~1095 and 625 cm^{-1} due to the $\nu_3(F_2)$ and the $\nu_4(F_2)$ modes of the uncoordinated ClO_4^-, respectively [51]. The broad character and signs of splitting of the band at ~1095 cm^{-1} indicate the involvement of the ClO_4^- ion in hydrogen bonding; this hydrogen bonding was established by X-ray crystallography (*vide supra*). The i.r. spectra of *(3)* in KBr and Nujol are different. The spectrum in KBr is indicative of the presence of ionic (uncoordinate) ClO_4^- groups (point group T_d), exhibiting the $\nu_3(F_2)$ and $\nu_4(F_2)$ vibrations at

Table 9. Most characteristic and diagnostic i.r. fundamentals (cm^{-1}) for DMU and its complexes *(1)–(4)*

Assignments	DMU	*(1)*	*(2)*	*(3)*	*(4)*
ν(NH)	3360–3348	~3365	3425–3345	3400–3340	3370–3350
ν(CO)	1628	1582	1580	1589	1597
$\nu_{as}(CN)_{amide} + \delta_{as}(NH)$	1591	1637	1636	1615	1623
δ_s(NH)	1541	1456	1453	1452	1451
$\delta_{as}(NH) + \nu_{as}(CN)_{amide}$	1270	1351	1358	1358	1357
$\nu_s(N{-}CH_3)$	1175	1180	1183	1180	1180
$\nu_{as}(N{-}CH_3)$	1040	1049	1050	1039	1036
π(CO)	775	770	766	767	770
δ(CO)	702	637	654	636	638

~1090 and 626 cm^{-1}, respectively. It was also observed that by pressing the KBr pellet the colour of the sample changes from blue to brown. The spectrum in Nujol exhibits two bands in the range of the stretching vibrations of the perchlorate group (at 1101 and 1060 cm^{-1}) and two in the range of the bending vibrations (at 655 and 620 cm^{-1}), as expected for monodentate perchlorato ligands (point group C_{3v}). The above spectroscopic observations suggest that the perchlorato ligands are replaced by bromides in the KBr matrix.

Concluding remarks and perspectives

The $M(ClO_4)_2 \cdot 6H_2O$/DMU chemistry (M = Mn, Ni, Cu, Zn) described here has fulfilled its promise as a source of interesting hydrogen-bonded networks based on simple metal complexes. It is important to note that complexes *(1)–(4)* were the only products to be isolated from the corresponding reaction mixtures in EtOH or Me_2CO, strongly suggesting that the reactions and crystallisations are selective. The great stability of the $[M(DMU)_6]^{2+}$ (M = Mn, Ni, Zn) cations in the solid state can be partly attributed to a pseudochelate effect. The strong intracationic hydrogen bonds present in the structures of *(1)*, *(2)* and *(4)* create a large number (six) of six-membered pseudochelating MOCNH···O rings per M^{II} atom, giving an extra stabilisation to the $[M(DMU)_6]^{2+}$ cation. This confirms the general rule (developed for organic compounds [7]) that six-membered intramolecular hydrogen bonds form in preference to intermolecular hydrogen bonds. The inability of copper(II) to form a $[Cu(DMU)_6]^{2+}$cation can be associated with its special $3d^9$ electronic configuration.

This work has confirmed that the hexakis(*N*,*N*′-dimethylurea)metal(II) cations can act as hydrogen-bonding building blocks with multi-fold connectivity linking perchlorate anions to generate an 1D architecture in the case of manganese(II) and two different 2D hydrogen-bonded networks in the cases of nickel(II) and zinc(II). We are presently pursuing our prediction that these cations will form hydrogen bonding contacts to a variety of anions to generate a rich diversity of networks. We have also shown that the hydrogen bonding functionalities on the molecules of tetrakis(*N*,*N*′-dimethylurea) bis(perchlorato)copper(II) have yielded a 2D architecture without the intervention of anionic intermediaries. We currently work on other neutral metal complexes of DMU using halides as co-ligands to take advantage of the facts that there is more space available for guest molecules and no possibility for unpredictable hydrogen bonding to the counterion.

There are two main motifs of intermolecular/interionic hydrogen bonds that have been observed in the structures of compounds *(1)–(4)*. These are N—H···O($OClO_3^-$/ClO_4^-) hydrogen bonds observed in all the four structures and C—H···O(ClO_4^-) weak interactions observed in *(2)* and *(4)*.

While both lone pairs on the carbonyl oxygen atom of free ureas act as hydrogen bond acceptors (Figure 1), in the metal complexes of DMU described here one pair acts as a hydrogen bond accceptor and the other participates in the formation of the metal–oxygen coordination bond. We do believe that *N*,*N*′-disubstituted ureas would become central players in the field of hydrogen-bonded networks of coordination complexes.

Acknowledgement

S.P.P. thanks the University of Antwerp for financial support.

References

1. P.S. Corbin, S.C. Zimmerman, P.A. Thiessen, N.A. Hawryluk and T.J. Murray, *J. Am. Chem. Soc.*, **123**, 10475 (2001).
2. J.-M. Lehn, *Supramolecular Chemistry Concepts and Perspectives*, VCH, Weinheim, 1995.
3. F. Vögtle, *Supramolecular Chemistry – An Introduction*, Wiley, Chichester, UK, 1991.
4. G.M. Whitesides, E.E. Simanek, J.P. Mathias, C.T. Sato, D.N. Chin, M. Mammen and M. Gordon, *Acc. Chem. Res.*, **28**, 37 (1995).
5. F.M. Raymo and J.F. Stoddart, *Curr. Opin. Colloid Interf. Sci.*, **1**, 116 (1996).
6. C.M. Paleos and D. Tsiourvas, *Angew. Chem., Int. Ed. Engl.*, **34**, 1696 (1995).
7. S. Subramanian and M.J. Zaworotko, *Coord. Chem. Rev.*, **137**, 357 (1994).
8. G.R. Desiraju, *Angew. Chem., Int. Ed. Engl.*, **34**, 2311 (1995).
9. D.C. Sherrington and K.A. Taskinen, *Chem. Soc. Rev.*, **30**, 83 (2001).
10. C.B. Aakeröy and K.R. Seddon, *Chem. Soc. Rev.*, **22**, 397 (1993).
11. J.M. Lehn, *Angew. Chem., Int. Ed. Engl.*, **29**, 1304 (1990).
12. G.R. Desiraju, *Crystal Engineering*: *The Design of Organic Solids*, Elsevier, Amsterdam, 1989.
13. A.D. Burrows, C.-W. Chan, M.M. Chowdry, J.E. McGrady and D.M.P. Mingos, *Chem. Soc. Rev.*, **24**, 329 (1995).
14. For an excellent recent review see: A.M. Beatty, *Cryst. Eng. Commun.*, **51**, 1 (2001).
15. A.J. Blake, P. Hubberstey, W.-S. Li, C.E. Russel, B.J. Smith and L.D. Wraith, *J. Chem. Soc., Dalton Trans.*, 747 (1998).
16. C.B. Aakeröy and A.M. Beatty, *Chem. Commun.*, 1067 (1998).
17. D.M.L. Goodgame, I. Hussain, A.J.P. White and D.J. Williams, *J. Chem. Soc., Dalton Trans.*, 2899 (1999).
18. E. Breuning, U. Ziener, J.-M. Lehn, E. Wegelius and K. Rissanen, *Eur. J. Inorg. Chem.*, 1515 (2001).
19. K.S. Min and M.P. Suh, *Chem. Eur. J.*, **7**, 303 (2001).
20. M. Tadocoro and K. Nakasuji, *Coord. Chem. Rev.*, **198**, 205 (2000).
21. P. Dastidar, Z. Stein, I. Goldberg and C.E. Strouse, *Supramol. Chem.*, **7**, 257 (1996).
22. M. Munakata, L.P. Wu, M. Yamamoto, T. Kuroda-Sowa and M. Maekawa, *J. Am. Chem. Soc.*, **118**, 3117 (1996).
23. C.B. Aakeröy, A.M. Beatty, D.S. Leinen and K.R. Lorimer, *Chem. Comm.*, 935 (2000).
24. N. Lalioti, C.P. Raptopoulou, A. Terzis, A. Panagiotopoulos, S.P. Perlepes and E. Manessi-Zoupa, *J. Chem. Soc., Dalton Trans.*, 1327 (1998).
25. S. De Beukeleer, G.S. Papaefstathiou, C.P. Raptopoulou, A. Terzis, S.P. Perlepes, H.O. Desseyn and E. Manessi-Zoupa, *Z. Naturforsch. b*, in press.

26. K. Skorda, G.S. Papaefstathiou, A. Vafiadis, A. Lithoxoidou, C.P. Raptopoulou, A. Terzis, V. Psycharis, E. Bakalbassis, V. Tangoulis and S.P. Perlepes, *Inorg. Chim. Acta*, **326**, 53 (2001).
27. G.S. Papaefstathiou, A. Tsohos, C.P. Raptopoulou, A. Terzis, V. Psycharis, D. Gatteschi and S.P. Perlepes, *Cryst. Growth Design*, **1**, 191 (2001).
28. G.S. Papaefstathiou, S.P. Perlepes, A. Escuer, R. Vicente, A. Gantis, C.P. Raptopoulou, A. Tsohos, V. Psycharis, A. Terzis and E.G. Bakalbassis, *J. Solid State Chem.*, **159**, 371 (2001).
29. V. Tangoulis, C.P. Raptopoulou, V. Psycharis, A. Terzis, K. Skorda, S.P. Perlepes, O. Cador, O. Kahn and E.G. Bakalbassis, *Inorg. Chem.*, **39**, 2522 (2000).
30. B. Moulton and M.J. Zaworotko, *Chem. Rev.*, **101**, 1629 (2001).
31. M.C. Etter, *Acc. Chem. Res.*, **23**, 120 (1990).
32. X.Q. Zhao, Y.L. Chang, F.W. Fowler and J.W. Lauher, *J. Am. Chem. Soc.*, **112**, 6627 (1990).
33. T.L. Nguyen, F.W. Fowler and J.W. Lauher, *J. Am. Chem. Soc.*, **123**, 11057 (2001).
34. J.W. Lauher, Y.L. Chang and F.W. Fowler, *Mol. Cryst. Liquid Cryst.*, **211**, 99 (1992).
35. S. Swaminathan and B.M. Graven, *Acta Crystallogr. B*, **40**, 300 (1984) and references cited therein.
36. R. Keuleers, H.O. Desseyn, B. Rousseau and C. Van Alsenoy, *J. Phys. Chem. A*, **104**, 5946 (2000).
37. R. Keuleers, H.O. Desseyn, B. Rousseau and C. Van Alsenoy, *J. Phys. Chem. A*, **103**, 4621 (1999).
38. R. Keuleers, G.S. Papaefstathiou, C.P. Raptopoulou, V. Tangoulis, H.O. Desseyn and S.P. Perlepes, *Inorg. Chem. Comm.*, **2**, 472 (1999).
39. R. Keuleers, G.S. Papaefstathiou, C.P. Raptopoulou, S.P. Perlepes and H.O. Desseyn, *J. Mol. Struct.*, **525**, 173 (2000).
40. R. Keuleers, J. Janssens and H.O. Desseyn, *Thermochim. Acta*, **354**, 125 (2000).
41. G.M. Sheldrick, *SHELXS-86*, Structure solving program, University of Göttingen, Germany, 1986.
42. G.M. Sheldrick, *SHELXS-93*, Crystal structure refinement, University of Göttingen, Germany, 1993.
43. E. Weber, I. Csöregh, J. Ahrendt, S. Finge and M. Czugler, *J. Org. Chem.*, **53**, 5831 (1988).
44. I. Csöregh, M. Czugler, A. Ertan, E. Weber and J. Ahrendt, *J. Incl. Phenom. Mol. Recognit. Chem.*, **8**, 275 (1990).
45. M. Tiliakos, P. Cordopatis, A. Terzis, C.P. Raptopoulou, S.P. Perlepes and E. Manessi-Zoupa, *Polyhedron*, **20**, 2203 (2001) and references cited therein.
46. L. Lebioda, *Acta Crystallogr. B*, **36**, 271 (1980) and references cited therein.
47. J. Delaunay and R.P. Hugel, *Inorg. Chem.*, **25**, 3957 (1986).
48. G. Galeazzi, U. Russo, G. Valle and S. Galogero, *Transition Met. Chem.*, **6**, 325 (1981).
49. M.C. Mattos, E. Surcouf and J.-P. Mornon, *Acta Crystallogr. B*, **33**, 1855 (1977).
50. F.A. Cotton and G. Wilkinson, *Advanced Inorganic Chemistry*, 5th edit., Wiley, New York, 1988.
51. K. Nakamoto, *Infrared and Raman Spectra of Inorganic and Coordination Compounds*, 4th edit., Wiley, New York, 1986.
52. J.P. Barbier and R.P. Hugel, *Inorg. Chim. Acta*, **24**, 1 (1977).

TMCH 5461